

## Article

# Operation Characteristics for the Superconducting Arc-Induction Type DC Circuit Breaker

Sangyong Park  and Hyosang Choi \*

Department of Electrical Engineering, Chosun University, Gwangju 61452, Korea; sangyong4400@gmail.com

\* Correspondence: hyosang@chosun.ac.kr; Tel.: +82-62-230-7025

Received: 19 June 2020; Accepted: 28 July 2020; Published: 30 July 2020



**Abstract:** The multi-terminal direct current network is expected to commercialize while carrying out projects related to DC power systems worldwide. Accordingly, it is necessary to develop a DC circuit breaker required for the DC power system. A DC circuit breaker should be developed to protect the DC power system and the consumer from the transient state on the line in any case. Currently, the use of power semiconductors increases the performance of DC circuit breakers. However, power semiconductors are expensive and suffer series of losses from frequent failures. Therefore, the DC circuit breaker must have a reliable, stable, and inexpensive structure. We proposed a new type of arc-induction type DC circuit breaker. It consists of a mechanical blocking contact, an induction needle and a superconducting magnet. It blows the arc with an induction needle using the Lorentz force according to the high magnetic field of the superconducting magnet. The arc-induction needle absorbs the arc and flows through the ground wire to the ground to extinguish the arc. We established this principle of arc induction as a mathematical model. In addition, the Maxwell program was used to secure data of electric and magnetic fields and apply them to mathematical models. The results obtained through numerical analysis were analyzed and compared. As a result, we confirmed that the magnitude of the force exerted on the electrons between the mechanical contacts with the superconducting magnets increased about 1.41 times and reasoned the arc-induction phenomenon out numerically.

**Keywords:** DC circuit breaker; arc-induction type; superconducting magnets; lorentz force

## 1. Introduction

With the rapid growth of IT-related industries worldwide, the penetration rate of big data is also increasing. As a result, digital data are becoming the center of the cloud in each field as well as in the cloud of each representative group. Due to this, the increase of the digital load is increasing. In addition, as the scope of the use of small-scale power generators formed based on renewable energy sources expands, various projects to increase the efficiency of electricity transmission and distribution by combining DC power sources distributed in each region into one DC grid are in progress. The expansion of the DC power grid will gradually increase. For this reason, the interest of voltage source converter (VSC)-based high-voltage DC (HVDC) and DC grids is inevitably increasing [1–4].

As the range of DC applications is widening worldwide, numerous projects are underway, from the single DC system to the multi DC system. In particular, in the DC-based modular multilevel converter (MMC) research, a method for cutting off the DC fault current is recently being studied [4]. In addition, studies such as DC fault-blocking schemes based on full-bridge sub-modules (FBRSM), clamp-double submodules (CDSM), and hybrid submodules have been proposed [5,6]. However, this method unconditionally requires a semiconductor switching device for a power system that has a fast operation characteristic. As a result, the economic efficiency is very low, and frequent failures of semiconductors have become a big problem. Something to replace the semiconductor has become

sought after, and a solution for this remains to be elucidated. As a result, it is very necessary to study the DC circuit breaker of the best protection scheme as a control method for the transient characteristic DC fault current occurring in the multi-terminal direct current (MTDC) network system.

The DC system is divided into HV (High Voltage), MV (Middle Voltage), and LV (Low Voltage). In HVDC, hybrid (semiconductor + mechanical contacts) circuit breakers have been developed and commercialized. In MV and LV, there is a problem of the cost burden of the semiconductor and the degradation power of the semiconductor. Therefore, research on mechanical DC circuit breakers is active in MV and LV distribution. Representatively, there is a study of DC circuit breakers using an arc chute. This is an arc extinguishing method that absorbs or dissipates the energy of the arc, and effective cutting-off techniques have been studied using special elements and magnets. However, the technology was not developed until the commercialization stage. If it fails to cut off DC fault current rapidly, all of the DC system will be blacked out under the influence of high fault current. To solve this problem, we proposed a DC circuit breaker method using an induction needle [5,6]. This is a model that applies an induction needle made by devising a lightning rod to a mechanical breaker contact. It is a method of extinguishing an arc generated between mechanical contacts using an induction needle when the line is in a transient state. There is a limit to the technique of inducing an arc by placing a simple induction needle. This is because the transient current blocking speed relies on the opening speed of the mechanical breaker. Therefore, a limit is recognized in the opening speed of the contact of the mechanical breaker, and a superconducting magnet is used to overcome this. The superconducting magnet generates a high magnetic field in a short time in a model that is relatively smaller than a normal magnet. In addition, it has the economic advantage of maintaining the superconducting state through low-cost liquid nitrogen. The superconducting magnets are located perpendicular to the contact point of the mechanical DC circuit breaker, creating a strong Lorentz force inside the contact point. It was judged that if the induction needle was placed in the direction of this force, arc-induction could be effectively achieved. Therefore, we tried to conduct a simulation study to observe the possibility of cutting-off operation of a superconducting arc-induction type DC circuit breaker. The superconducting magnet and arc-induction type DC circuit breaker, which are the components of the model, were modeled through the Maxwell program and we utilized an optometrics technique. This can derive and analyze the predicted electric and magnetic field values according to the open motion movement based on the mechanical cutting-off contact model. Based on these data, we tried to analyze the characteristics of the arc occurring in the blocking section by using the proven theoretical formula [7,8]. This is one of the basic studies that can confirm the blocking characteristics of the idea based on the proven theory and the combination of mechanical elements before making a prototype.

## 2. Background

### *Superconducting Arc-Induction Type DC Circuit Breaker Structure and Principle*

Figure 1 shows the structure of the superconducting arc-induction DC circuit breaker. The mechanical contacts (a) and (b) are the anode (+) and cathode (−). The anode is a fixed electrode, and the cathode is a movable electrode. (c) is an induction needle, which induces arcs from the between mechanical contacts and extinguishes them by flowing them to the ground through a ground wire. (d) is a superconducting cooling vessel, in which a superconducting magnet is constructed. It is positioned on either side of the central mechanical contacts. It emits magnetic flux density  $B$  [tesla] in the same direction. (e) is a virtual criterion plane for explanation of the principle and numerical analysis, and  $S$  [m<sup>2</sup>]. (c) is proposed in the shape of a lightning arrester with an induction needle and plays a role. The process of lightning occurrence is as follows. As the cloud develops, electric charges are generated, and separately accumulated in each part, increasing its capacity. When the amount of accumulated electric charges increases and reaches a certain value, a strong electric field is formed, thereby causing a discharge phenomenon. Lightning rods are used to prevent line breakdowns by the

falling of a thunderbolt. This is similar to the arc resulting from the blocking action of a mechanical DC circuit breaker. A strong electric field between the anode and the cathode is generated by the mechanical contact opening operation, thereby forming an arc plasma through repetition of excitation and ionization of electrons. Therefore, the arc-induction type DC circuit breaker has a blocking principle that assists the fast-breaking operation of the main line by inducing the arc energy generated between the blocking contacts. Here, the superconducting magnet generates a high magnetic field and blows the arc to the induction needle through the Lorentz force. The two mechanism are common in a same way that are the protecting principle for bypass the path of high energy at the moment using a needle with a strong field strength. The differences are as follows. Lightning has an unspecified path and very strong energy. DC arc has unstable energy, but the path to occur is predictable. In addition, it releases controllable energy.

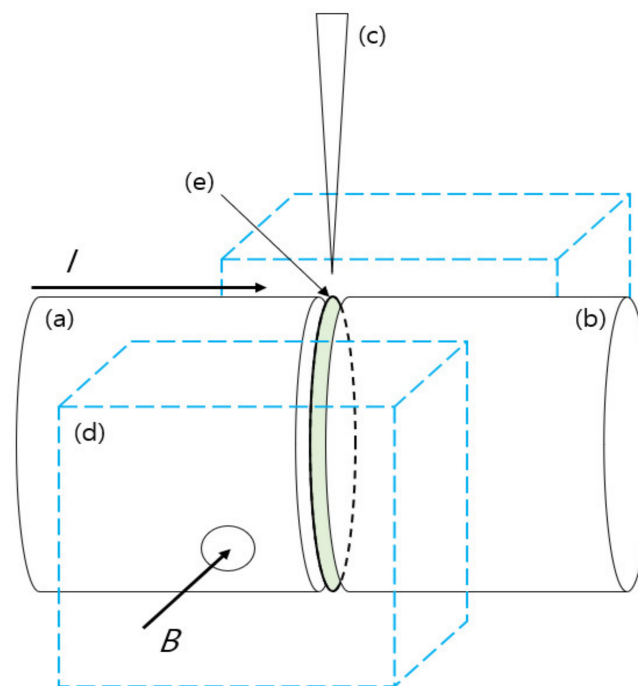


**Figure 1.** Configuration diagram of superconducting arc-induction type DC circuit breaker (arc breaking part). a—Anode; b—Cathode; c—Induction needle; d—Superconducting magnets; e—Virtual criterion plane.

Figure 2 shows the configuration and mechanism of a superconducting arc-induction type DC circuit breaker. Figure 2a is normal state, and the mechanical cutting-off contact is closed. At this time, the steady current  $I$  [A] flows through the contacts. In addition, the induction needle and the superconducting magnet do not negatively affect the steady current flowing through the primary line. Figure 2b shows a transient state (1st) and shows the point at which opening of the cutoff contact has started. When the contact is opened, electrons escape due to the rapidly rising electric field at the surface of conductor. Excitation and ionization phenomena are generated by the escaped electrons, and inelastic collisions with gaseous electrons continue to occur rapidly. These phenomena gather to form an arc plasma, and a fault current is generated between the contacts. Figure 2c shows a transient state (2nd) and is the point at which opening of the cutoff contact has been made to some extent. At this time, the arc is subjected to Lorentz force under the influence of the magnetic field of the superconducting magnet, and the direction is the point where the guide needle is located. Eventually, the arc is guided to the guide needle and flows out to the ground along the ground wire to extinguish it. Figure 2d shows a transient state (3rd), the completion of blocking at the time when the opening of the blocking contact is completed.

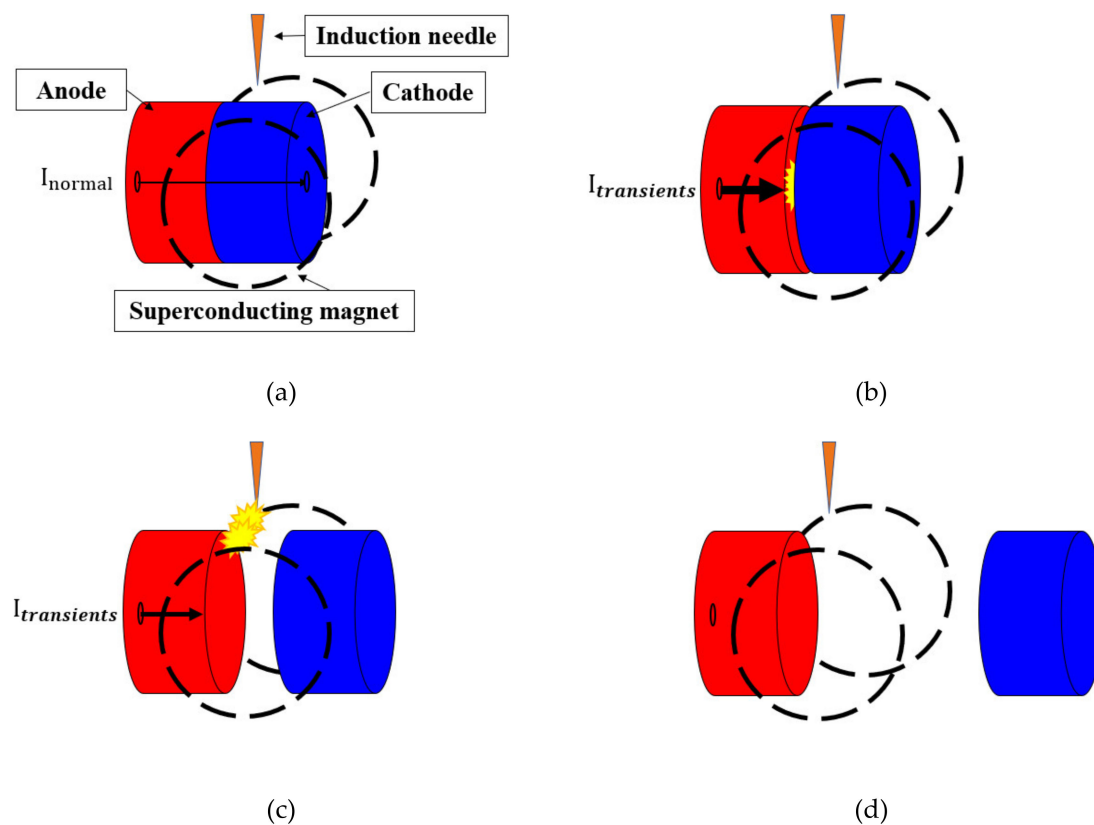


**Figure 2.** Operation mechanism of superconducting arc-induction type DC circuit breaker. (a) Normal state; (b) Transient state (1st); (c) Transient state (2nd); (d) Transient state (3rd).

The superconducting magnet is divided into DC field and pulse type. In the DC field type, the superconducting DC field type bulk magnet constantly generates a high magnetic field after being magnetized by an electromagnet. The pulse type instantaneously generates a high magnetic field for up to several tens of milliseconds [ms]. However, the pulse type is a structure that generates a high magnetic field in a short time through a superconducting wire, however, has a bed point. The superconductor pulse type requires an auxiliary current source. Fast current application must be made from the auxiliary current source in the transient state of the line. Since the timing at which the high magnetic field is generated is about several tens of milliseconds [ms], there is a time difference from the starting time of the accident to the starting time of the generating high magnetic field. Therefore, at the time of the accident, the operating of the superconductor pulse type has a time delay. In this paper, a DC-field type bulk superconducting magnet is used. It maintains a superconducting state at a low temperature to generate a high magnetic field and does not require additional equipment. Bulk-type superconducting magnets can generate magnetic fields up to 5 [T]. We applied a face-to-face type superconducting bulk magnet to an arc-induction type DC circuit breaker. The Y123 bulk superconductor is a simulation of a magnetized model using the Iteratively Magnetizing pulsed-field operation with Reducing Amplitudes (IMRA) method [9].

### 3. Mathematical Analysis

In this paper, the phenomenon of the arc generated in the arc-induction type DC circuit breaker and the high magnetic field characteristics generated by the superconducting magnet were analyzed by an electromagnetic field simulation. In addition, based on the simulation results, we derived the arc-induced characteristics using the Lorentz force equation.

### 3.1. Mathematical Model

Figure 3 shows the force received by the electrons between the mechanical contacts when the contacts are open.  $\vec{F}_E$  is the electrical force,  $\vec{F}_M$  is the Magnetic force, and 'N' is a free electron. The anode and cathode appear as (+) and (−). A free electron is located inside the electrical field generated by between the mechanical contacts and magnetic field. When the contacts are open, the free electron is received  $\vec{F}_E$  and  $\vec{F}_M$  at the same time.  $\vec{F}_L$  is the Lorentz force for vector sum of the  $\vec{F}_E$  and  $\vec{F}_M$ .

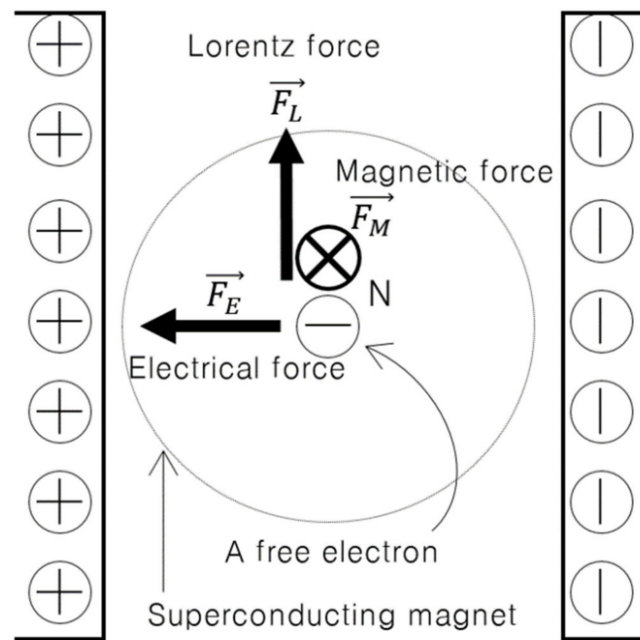


**Figure 3.** Forces received to the free electrons between mechanical contacts at the opening state.

In the normal state, the blocking contacts (anode and cathode) are closed, and the normal current  $I_{normal}$  flows. This can be expressed as Equation (1) as the flow of free charge per unit time.

$$I_{normal} = \frac{Q_{normal}}{t_{normal}} [A] \quad (1)$$

If  $N_{normal}$  is the total number of electrons that have passed through the reference plane  $S$  for  $t_{normal}$  seconds, then the total amount of charge  $Q_{normal}$  is expressed by Equation (2).

In this paper, assuming that the motion of the electron is a constant velocity motion, the total volume of electrons passing from the reference plane  $S$  in Figure 1e for  $t_{normal}$  seconds is  $S\vec{v}_{normal}t_{normal}$ . If the number of free electrons per unit volume is  $n_e$ , the total number of electrons in  $S\vec{v}_{normal}t_{normal}$  is expressed by Equation (3).

$$Q_{normal} = qN_{normal} \quad (2)$$

$$N_{normal} = S\vec{v}_{normal}t_{normal}n_e \quad (3)$$

Summarizing Equations (1)–(3) provides Equation (4).

$$I_{normal} = \frac{Q_{normal}}{t_{normal}} = \frac{qN_{normal}}{t_{normal}} = \frac{q(S\vec{v}_{normal}t_{normal}n_e)}{t_{normal}} = S\vec{v}_{normal}qn_e [A] \quad (4)$$

In the transient state, the blocking contact opens, and an arc occurs. Here, the high magnetic field of the superconducting magnets should be considered. If the sum of the forces received by the free

electrons of the arc is  $\vec{F}$ , this becomes Equation (5), and if the total number of free electrons of the arc is  $N_{transients}$ , then the Lorentz force  $\vec{f}$  according to Equation (6).

$$\vec{F} = Q_{transients}(\vec{E} + \vec{v}_{transients} \times \vec{B}) \text{ [N]} \quad (5)$$

$$\vec{f} = \frac{Q_{transients}(\vec{E} + \vec{v}_{transients} \times \vec{B})}{N_{transients}} \text{ [T]} \quad (6)$$

The volume ( $V$ ) of the arc according to the reference plane ( $S$ ) and the distance ( $L$ ) becomes Equation (7).

$$V = SL \text{ [m}^3\text{]} \quad (7)$$

Therefore, in the transient state, the arc  $I_{transients}$  becomes Equation (8). According to Equation (7), the number of free electrons included in the volume of the arc can be obtained from Equation (10) by put Equation (9) into Equation (6).

$$I_{transients} = S\vec{v}_{transients}qn_e \text{ [A]} \quad (8)$$

$$N_{transients} = SLn_e \quad (9)$$

$$\vec{f} = \frac{Q_{transients}(\vec{E} + \vec{v}_{transients} \times \vec{B})}{N_{transients}} = q(\vec{E} + \vec{v}_{transients} \times \vec{B}) \text{ [N]} \quad (10)$$

Consequently, Equation (11) is the Lorentz force, which is obtained from the vector product of the electron movement speed  $\vec{v}_{transients}$  of Equation (10) and the magnetic field  $\vec{B}$ . In this paper, since the electron movement speed can be viewed as the speed of light, the value of  $2.99792458 \times 10^8$  [ms] was applied.

$$\vec{f} = q(\vec{E} + |v_{transients}||B|\sin\theta) \text{ [N]} \quad (11)$$

### 3.2. Simulation Design

Figure 4 shows the superconducting arc-induction type DC circuit breaker modeled using the Maxwell 3D program. (a) is the anode, (b) is the cathode, and (c) is the induction needle. (d) represents the superconducting magnets. The superconducting magnet had a distance from the mechanical contact of about 10 mm [10]. The simulation model used in this paper was redesigned by reducing the size and area by using a superconducting bulk magnet material capable of generating a high magnetic field up to 5 [T]. Sources of superconducting magnets are not presented in the Maxwell program. Therefore, we applied a superconducting model of material by preceding research information [11]. This was a superconducting magnet to which a ferromagnetic element was applied, which was the result of a previous study that solved the Brandt algorithm and the Campbell equation using the finite element method [12,13]. The rated voltage was set as anode 300 [V], cathode 0 [V], and induction needle 0 [V]. Table 1 shows the elements according to the design parameters of simulation model [14,15]. As the simulation data, the data were analyzed using the Maxwell program's optimetrics function. Since the electric and magnetic fields were analyzed at intervals of 1 mm, the cutting-off characteristics can be predicted by applying the driving speed of the prototype circuit breaker based on this data. Through this analysis technique, it is possible to see the possibility of the blocking operation of the model in the process of preparing the prototype.

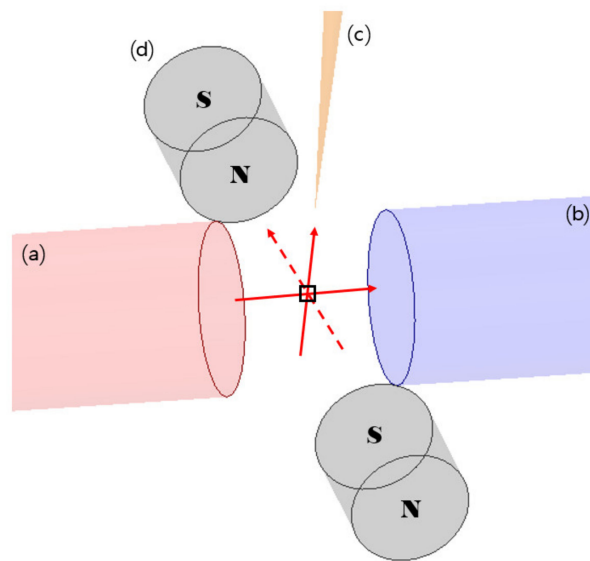


**Figure 4.** Maxwell simulation model of superconducting arc-induction type DC circuit breaker. a—Anode; b—Cathode; c—Induction needle; d—Superconducting magnets.

**Table 1.** Design parameters of simulation model.

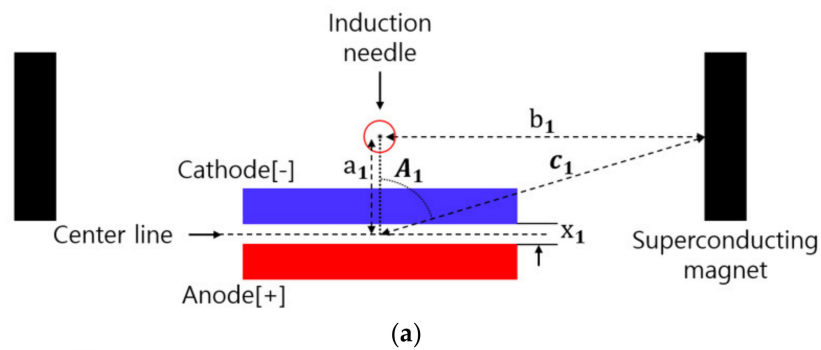
Composition	Resource	Value
Contacts [Anode and Cathode]	Material	Copper [Cu]
	Radius [mm]	5
	Length [mm]	150
Induction needle	Material	Copper [Cu]
	Radius [mm] (bottom)	0
	Radius [mm] (top)	1
	Height [mm]	25
Superconducting magnets	Type	Bulk(DC field)
	Height [mm]	8
	Radius [mm]	3.45
	Magnitude [kA/m]	5200
	X component	1

### 3.3. Numerical Analysis Domains and Conditions

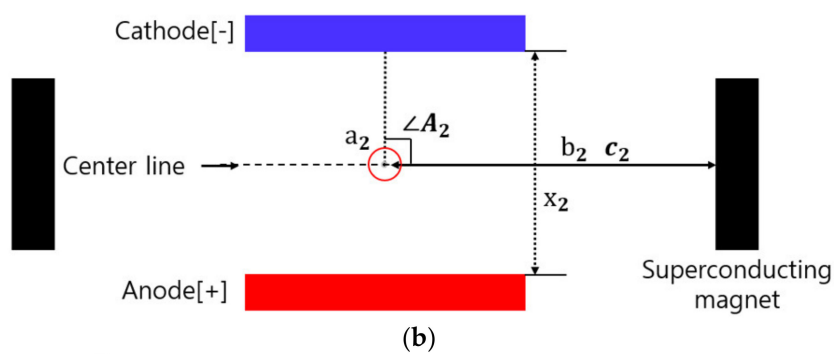
Figure 5 shows the numerical values for the distance and angle of each element of the arc-induced DC circuit breaker according to the gap of the contacts. This is a simulation model to check the changes in the electric flux density  $\vec{E}$  and the magnetic field  $\vec{B}$  generated by the superconducting magnet according to the opening operation of the blocking contacts. The fixed pole, the anode, is located at the bottom, and the movable pole, the cathode, is located at the top. Superconducting magnets are located on the right and left sides with respect to the blocking contacts. The pole spacing was simulated from 0 mm up to 50 mm every 0.5 mm.  $x$  is the distance between the anode and cathode.  $a$  is the distance from the midpoint of the anode and cathode to the induction needle.  $b$  is the distance between the induction needle and the superconducting magnets.  $c$  is the distance from the midpoint of the anode and cathode to the superconducting magnets.  $\angle A$  is the angle  $\theta$  between the electric field  $\vec{E}$  and the magnetic field  $\vec{B}$ .



&lt; case 1 &gt;



&lt; case 2 &gt;



&lt; case 3 &gt;

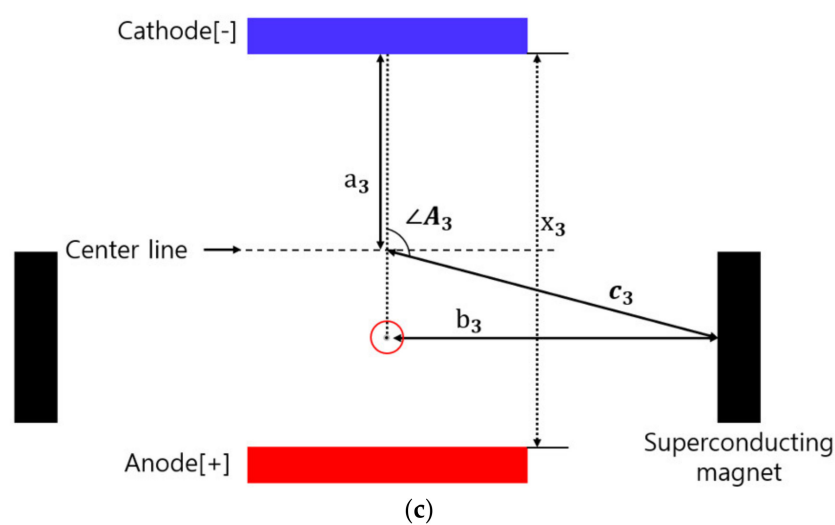


**Figure 5.** Mathematical indicators of arc-induction type DC circuit breakers according to the gap between the contacts (a) 0.5 mm, (b) 10 mm, (c) 30 mm.



Figure 5a shows the configuration when the pole spacing  $x_1$  is 0.5 mm.  $a_1$  is 4.75 mm.  $b_1$  is 15 mm and  $c_1$  is 15.734 mm.  $\angle A_1$  is  $72.428^\circ$ . Figure 5b shows the configuration when the pole spacing  $x_2$  is 10 mm.  $a_2$  is 0 mm.  $b_2$  and  $c_2$  are 15 mm.  $\angle A_2$  is  $90^\circ$ . Figure 5c shows the configuration when the pole spacing  $x_3$  is 50 mm.  $a_3$  is 25 mm, and  $b_3$  and  $c_3$  are 15 mm and 32.818 mm, respectively.  $\angle A_3$  is  $72.428^\circ$ .

Figure 6 graphically shows the electric field  $\vec{E}$  and the magnetic field  $\vec{B}$  generated according to the distance between poles. The reference points for measuring the electric and magnetic fields are the center point of the center line shown in Figure 5. In addition, the high magnetic field strength of the superconducting magnet generated at the position of center point in Figure 6 was about 2.38 [T]. When the gap is 0.5 mm, the opening of the anode and cathode begins. The electric field was the highest at about  $4.39 \times 10^{17}$  [V/m], and the magnetic field was 2.14 [T]. When the pole distance is 10 mm, it represents the time when the movable pole cathode deviates between the superconducting magnets. The electric field was sharply lowered to  $7.94 \times 10^{16}$  [V/m], and the magnetic field was 2.38 [T] to be higher than before. The reason for the increased magnetic field is that it is not disturbed by the location of the cathode. When the pole spacing was 30 mm, the electric field was  $3.58 \times 10^{16}$  [V/m] and the magnetic field was 1.70 [T].

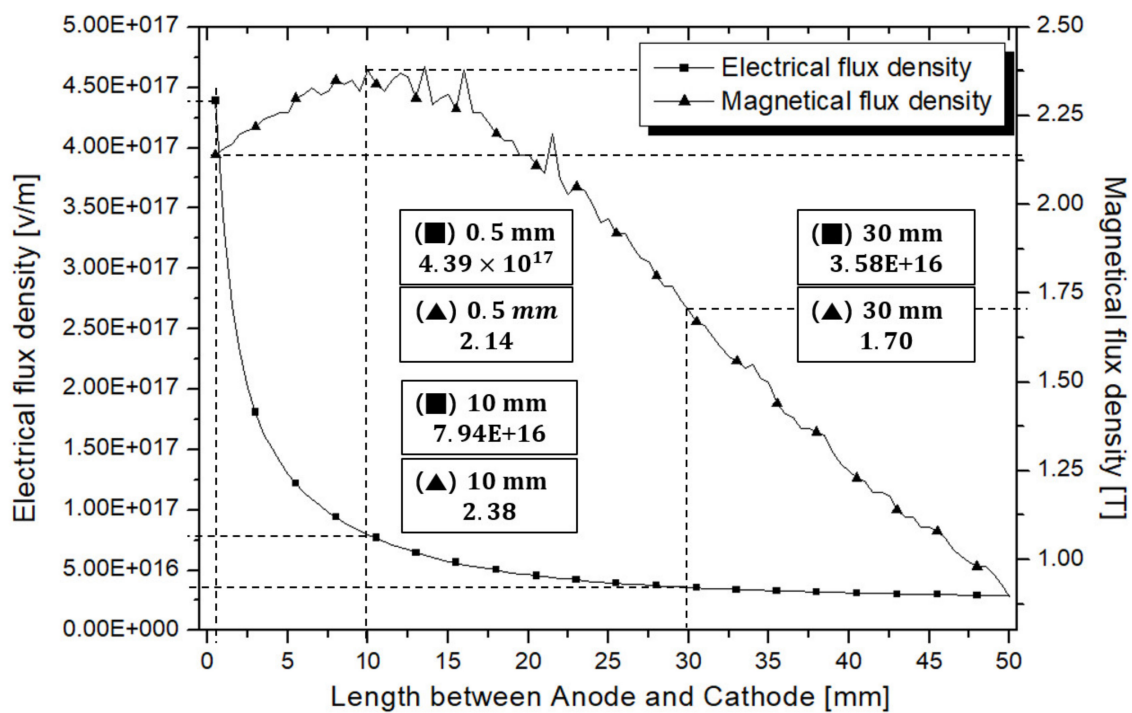


Figure 6. Electric field and magnetic field distributions according to the distance between poles.

### 3.4. Results of Mathematical Analysis

Figure 7 compares the force of the electric field and the magnetic field generated between the anode and the cathode according to the change of the pole spacing and graphs the results of the Lorentz force. At the cutting-off contact of the superconducting arc-induction type DC circuit breaker, there is a force of the electric field and magnetic force according to the open operation. Free electrons in arc energy are affected by two forces, and the direction and speed of movement are determined. Therefore, the force received by the electron is determined by the Lorentz force according to these two forces. Table 2 derives the force received by the electron by the electric field in the electric field equation through

Equations (12)–(14) based on the simulation result data when the pole spacing is 0.5, 5, 10, 15, 20 mm.  $\vec{F}_E$  is the force of the electric field,  $\vec{F}_M$  is the force of the magnetic field and  $\vec{f}$  is the Lorentz force.

$$\text{Electronic force [N]} \quad \vec{F}_E = q \cdot \vec{E} \quad (12)$$

$$\text{Magnetic force [N]} \quad \vec{F}_M = q(|v_t||B|\sin\theta) \quad (13)$$

$$\text{Lorentz force [N]} \quad \vec{f} = q(\vec{E} + |v_t||B|\sin\theta) \quad (14)$$

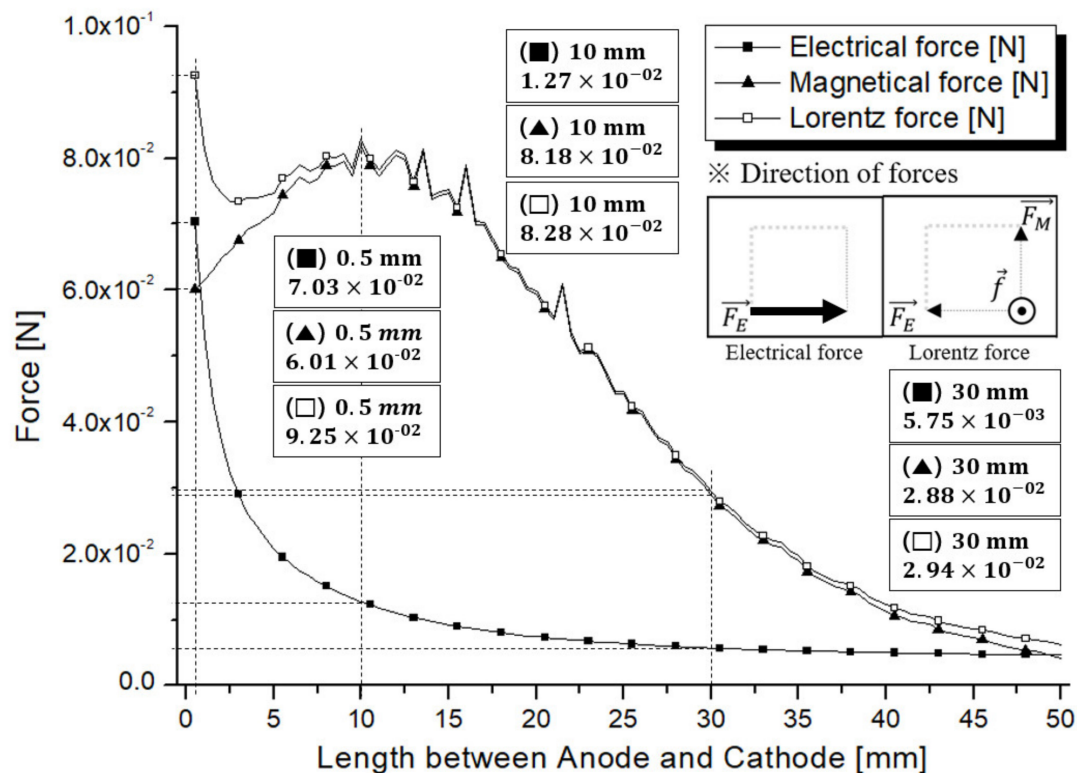


Figure 7. Comparison graphs of electric force, Magnetic force and Lorentz force.

Table 2. Electrical force, Magnetic force, and Lorentz force according to the length between anode and cathode.

Length between Anode and Cathode [mm]	Electrical Force [N] ( $\vec{F}_E$ ) [ $\rightarrow$ ]	Magnetical Force [N] ( $\vec{F}_M$ ) [ $\odot$ ]	Lorentz Force [N] ( $\vec{f}$ ) [ $\uparrow$ ]
0.5	$7.03 \times 10^{-2}$	$6.01 \times 10^{-2}$	$9.25 \times 10^{-2}$
5	$2.07 \times 10^{-2}$	$7.18 \times 10^{-2}$	$7.47 \times 10^{-2}$
10	$1.27 \times 10^{-2}$	$8.18 \times 10^{-2}$	$8.28 \times 10^{-2}$
15	$9.17 \times 10^{-3}$	$7.47 \times 10^{-2}$	$7.52 \times 10^{-2}$
30	$5.75 \times 10^{-3}$	$2.88 \times 10^{-2}$	$2.94 \times 10^{-2}$

As a result, when the length of between the anode and cathode was 0.5 mm, the force of the electric field was  $7.03 \times 10^{-2}$  [N], and the force of the magnetic field was  $6.01 \times 10^{-2}$  [N]. When the length between the contacts was 10 mm, the electric force was  $1.27 \times 10^{-2}$  [N] and the magnetic force was  $8.18 \times 10^{-2}$  [N]. When the gap was 30 mm, the electric force was  $5.75 \times 10^{-3}$  [N] and the magnetic force was  $2.88 \times 10^{-2}$  [N]. The Lorentz forces were  $9.25 \times 10^{-2}$  [N],  $8.28 \times 10^{-2}$  [N], and  $2.94 \times 10^{-2}$  [N] when the gap spacing was 0.5 mm, 10 mm, and 30 mm, respectively. When the gap was about 10 mm,

it was confirmed that the largest Lorentz force was generated at the time when the magnetic force was emitted 100%. This point of view was interpreted as the second case in Figure 5, and the same tendency was observed in simulation according to the theory.

Figure 8 shows the results data divided into type A and type B depending on the presence or absence of a superconducting magnet. Type A is a model without superconducting magnet applied to the existing arc-induction type DC circuit breaker. Type B is a model in which a superconducting magnet is applied to an arc-induction type DC circuit breaker. The simulation operation parameters are the measurement reference points, Figure 1e, according to the pole spacing, and were performed under the same conditions.

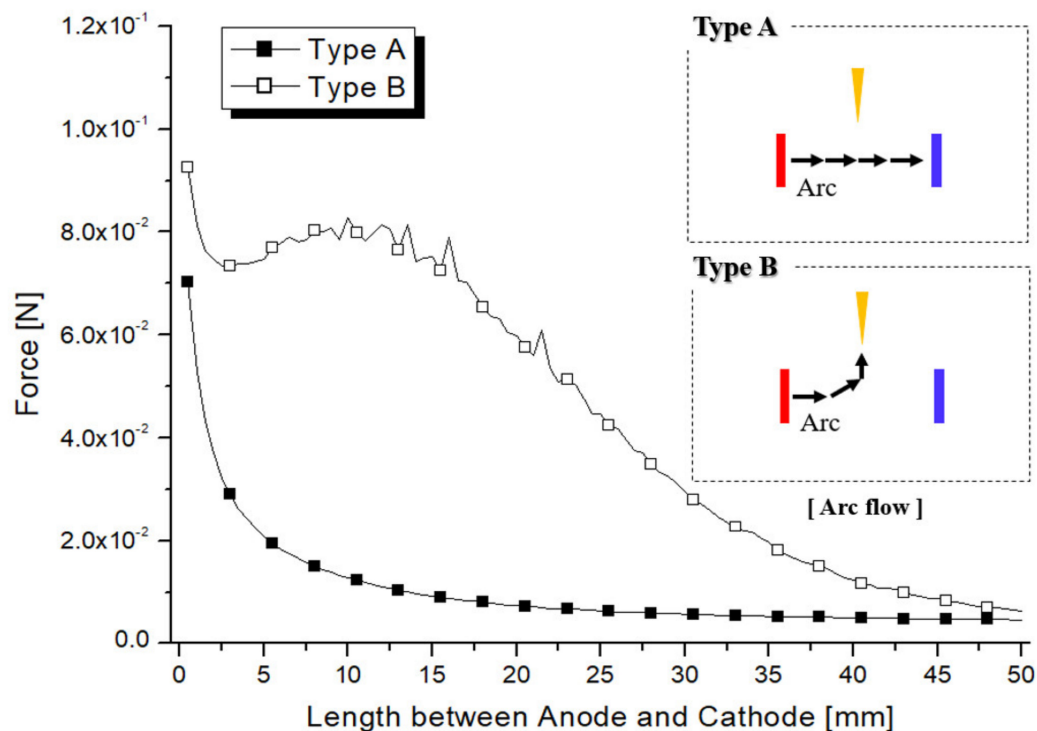


**Figure 8.** Graphs of the force received by an electron with or without the superconducting magnets.

As a result, for type A, the force received by the electron according to the pole spacing 0.5/10/30 mm is about  $7.03 \times 10^{-2}$  [N]/ $1.27 \times 10^{-2}$  [N]/ $5.75 \times 10^{-3}$  [N], and for type B, a force received is about  $9.25 \times 10^{-2}$  [N]/ $8.28 \times 10^{-2}$  [N]/ $2.94 \times 10^{-2}$  [N]. The force received by type A and B electrons differed approximately 1.31/6.52/5.11 times depending on the pole spacing 0.5/10/30 mm. The main difference between types A and B is the direction of the force. The direction of the force of type A is directed from the anode to the cathode, and the direction of the force of type B is directed from the anode to the induction needle by the Lorentz force.

When the pole spacing is less than 10 mm, the cathode is opened, and since it exists in a path where a high magnetic field of a superconducting magnet is generated, it is difficult for the Lorentz force to occur 100%. The highest force occurred at a pole spacing of 0.5 mm, but the direction of the force was from the anode to the cathode. Therefore, it can be explained based on the data in Figures 7 and 8 that the Lorentz force was highest when the pole spacing was 10 mm.

#### 4. Conclusions

We tried to prove the new DC cutting-off technology through simulations based on scientific equations. The arc-induction type DC circuit breaker is a new DC arc cutting-off method that extinguishes the arc generated by the contacts opening operation through the induction needle.

A superconducting magnet was used to increase the induction efficiency of the arc, and the type was designed as a bulk type. First, the principles and mechanisms of a superconducting arc-induction type DC circuit breaker were described based on the equation of Lorentz force. In addition, a simulation model of a superconductor and a DC circuit breaker was designed using the Maxwell program, and the values of electric and magnetic flux density were derived according to the spacing variable between the breaking contacts.

The arc occurs between the contacts according to the opening operation of the mechanical contact. In this arc, we wanted to confirm the phenomenon of free electron movement caused by the presence or absence of a superconducting magnet. In addition, an attempt was made to predict the motion of the arc under the influence of the force received by the free electron at the reference point. As a result, we designed a simulation model using physical values, and confirmed the strength of the electric field and the strength of the magnetic field caused by changes in the gap spacing. In addition, the phenomenon that the Lorentz force changes according to the data of the two forces was numerically confirmed. Based on this, it was possible to confirm the operating characteristics of the superconducting arc-induced DC circuit breaker. Finally, before we conducted the DC circuit breaker experiment, we were able to use the simulation to review the new idea and the reliability of the structure of the blocking contact.

**Author Contributions:** Conceptualization, S.P.; Data curation, S.P.; Formal analysis, S.P.; Funding acquisition, H.C.; Investigation, S.P.; Methodology, S.P.; Project administration, H.C.; Resources, S.P.; Software, S.P.; Supervision, H.C.; Validation, H.C.; Visualization, S.P.; Writing—original draft, S.P.; Writing—review & editing, H.C. All authors have read and agreed to the published version of the manuscript.

**Funding:** This research received no external funding.

**Acknowledgments:** This research was supported by Korea Electric Power corporation [grant number: R16XA01], this study was supported by research fund from Chosun University, 2020.

**Conflicts of Interest:** The authors declare no conflict of interest.

## References

1. Jia, H.; Yin, J.; Wei, T.; Huo, Q.; Li, J.; Wu, L. Short-Circuit Fault Current Calculation Method for the Multi-Terminal DC Grid Considering the DC Circuit Breaker. *Energies* **2020**, *13*, 1347. [\[CrossRef\]](#)
2. Li, Z.; He, Y.; Zhang, T.Q.; Zhang, X.P. Universal Power Flow Algorithm for Bipolar Multi-Terminal VSC-HVDC. *Energies* **2020**, *13*, 1053. [\[CrossRef\]](#)
3. Molina, M.J.P.; Larruskain, D.M.; Lopez, P.E.; Etxegarai, A. Analysis of Local Measurement-Based Algorithms for Fault Detection in a Multi-Terminal HVDC Grid. *Energies* **2019**, *12*, 4808. [\[CrossRef\]](#)
4. Liu, Y.; Zhang, L.; Liang, H. DC Voltage Adaptive Droop Control Strategy for a Hybrid Multi-Terminal HVDC System. *Energies* **2018**, *12*, 380. [\[CrossRef\]](#)
5. Park, S.Y.; Choi, H.S. Operating Characteristics of Arc-Induction Type DC Circuit Breaker. *Trans. KIEE* **2018**, *67*, 981–986.
6. Park, S.Y.; Choi, H.S. Characteristics of Arc-Induction Type DC Circuit Breaker Depending on Alteration of Induction Needle. *J. Elect. Eng. Technol.* **2020**, *15*, 279–285. [\[CrossRef\]](#)
7. Kim, H.S. Arcing Characteristics on Low-Voltage DC Circuit Breakers. *IEEE EPE Conf.* **2013**, *15*, 1–7.
8. Li, Y.; Yan, H.; Massoudi, M.; Wu, W.T. Effects of Anisotropic Thermal Conductivity and Lorentz Force on the Flow and Heat Transfer of a Ferro-Nanofluid in a Magnetic Field. *Energies* **2017**, *10*, 1065. [\[CrossRef\]](#)
9. Yokoyama, K.; Oka, T.; Okada, H.; Fujine, Y.; Chiba, A.; Noto, K. Solid-Liquid Magnetic Separation Using Bulk Superconducting Magnets. *IEEE Trans. Appl. Supercond.* **2003**, *13*, 1592–1595. [\[CrossRef\]](#)
10. Lee, S.M.; Kim, H.S. *A Study on Low-Voltage DC Circuit Breakers*; IEEE International Symposium on Industrial Electronics (ISIE): Taipei, Taiwan, 2013; pp. 1–6.
11. Philippe, M.P.; Fagnard, J.F.; Kirsch, S.; Xu, Z.; Dennis, A.R.; Shi, Y.H.; Cardwell, D.A.; Vanderhyden, B.; Vanderbemden, P. Magnetic Characterisation of Large Grain, Bulk Y-Ba-Cu-O Superconductor-Soft Ferromagnetic Alloy Hybrid Structures. *Phys. C Supercond.* **2014**, *502*, 20–30. [\[CrossRef\]](#)
12. Brandt, E.H. Superconductor Disks and Cylinders in an Axial Magnetic Field. I. Flux Penetration and Magnetization Curves. *Phys. Rev. B* **1998**, *58*, 6506–6522. [\[CrossRef\]](#)

13. Campbell, A.M. A New Method of Determining the Critical State in Superconductors. *Supercond. Sci. Technol.* **2007**, *20*, 292–295. [[CrossRef](#)]
14. Fujishiro, H.; Fujiwara, A.; Tateiwa, T.; Oka, T.; Hayashi, H. New Type Superconducting Bulk Magnet by Pulse Field Magnetizing with Usable Surface on both Sides in Open Space. *IEEE Trans. Appl. Supercond.* **2006**, *2*, 1080–1083. [[CrossRef](#)]
15. Yokoyama, K.; Igarashi, R.; Togasaki, R.; Oka, T. Improvement of the Trapped Field Performance of a Holed Superconducting Bulk Magnet. *IEEE Trans. Appl. Supercond.* **2015**, *25*, 1–4. [[CrossRef](#)]



© 2020 by the authors. Licensee MDPI, Basel, Switzerland. This article is an open access article distributed under the terms and conditions of the Creative Commons Attribution (CC BY) license (<http://creativecommons.org/licenses/by/4.0/>).